LASER INTERFEROMETER GRAVITATIONAL WAVE OBSERVATORY
- LIGO -
CALIFORNIA INSTITUTE OF TECHNOLOGY
MASSACHUSETTS INSTITUTE OF TECHNOLOGY

Engineering Note	**LIGO-E1500358-v1**

Preliminary Design Documents for Squeezing in Advanced LIGO

J. Miller, F. Matichard, E. Oelker, G. Mansell, M. Tse, A. Fernandez-Galiana, L Barsotti, P. Fritschel, M Evans

This is an internal working note of the LIGO project.

California Institute of Technology
LIGO Project, MS 18-34
Pasadena, CA 91125
Phone (626) 395-2129
Fax (626) 304-9834
E-mail: info@ligo.caltech.edu

Massachusetts Institute of Technology
LIGO Project, Room NW17-161
Cambridge, MA 02139
Phone (617) 253-4824
Fax (617) 253-7014
E-mail: info@ligo.mit.edu

LIGO Hanford Observatory
Route 10, Mile Marker 2
Richland, WA 99352
Phone (509) 372-8106
Fax (509) 372-8137
E-mail: info@ligo.caltech.edu

LIGO Livingston Observatory
19100 LIGO Lane
Livingston, LA 70754
Phone (225) 686-3100
Fax (225) 686-7189
E-mail: info@ligo.caltech.edu

WWW: http://www.ligo.caltech.edu/

Contents

1 Executive Summary

This document presents a Preliminary Design of a proposed new Advanced LIGO subsystem (SQZ), to allow for injection of squeezed light in Advanced LIGO.

The proposed design targets 3 dB of high frequency squeezing, equivalent to a $\sqrt{2}$ improvement in shot noise, and aims to be beneficial to Advanced LIGO during "low-power operations" (up to 200 kW of light stored in the arm cavities, currently corresponding to 50 W of laser light delivered by the PSL).

With Advanced LIGO operating at low power and with modest amount of squeezing, squeezed light injection is nearly equivalent to power increase, as the impact of radiation pressure produced by anti-squeezing is comparable to other low frequency noises. In other words, operating the current Advanced LIGO detectors at 50 W of input power is equivalent to operating at 25W with 3dB of squeezing. Moreover, adding 3 dB of squeezing to a detector operating at 50 W is still advantageous (see Appendix B).

The equivalence between squeezed light and power increase is broken for intra-cavity powers higher than 200 kW: at that point anti-squeezing imposes high levels of radiation pressure noise, and the benefit from squeezed light at high frequency is paired with an undesirable decrease in low-frequency performance.

For this reason, this proposed design must be considered as the first step toward a more complete squeezed light injection system (described in section 4) involving: a filter cavity to produce frequency dependent squeezing, an improved mode matching system, a lower-loss squeezed light injection path and an improved interferometer readout to increase the amount of measured squeezing.

The design shown in this document has therefore been conceived to be compatible with a multi-stage upgrade process.

In particular:

- the squeezed light source itself is able to produce high levels of squeezing; the modest level of measured squeezing quoted here, 3 dB, is due to lossy optical components (for example the Output Faraday Isolator) and the interferometer readout photo-detectors. These items can be improved at a later time.
- the filter cavity set-up is nearly independent from the production of squeezed light, it can be added at a later date with only minor modification of the optical layout (the squeezed beam will reflect off the filter cavity before being injected into the interferometer).

A budget associated with the proposed design will be circulated at the time of the review.

In parallel, the planned R&D program to finalise a complete design involving a filter cavity will be carried forward at LASTI (see T1500488).

A tentative timeline for delivering a squeezed light source to one of the LIGO site (specifically, Livingston) is described in Appendix 10.

2 Motivations and Context

After successful implementation in LIGO and GEO, squeezed light is a promising technology for improving the sensitivity of Advanced LIGO. The LIGO Laboratory, together with several LSC groups, is working to complete the design of a frequency dependent squeezed light source capable of producing at least 6dB of squeezing at high frequency (thus improving high-frequency noise by a factor of 2) without degrading low-frequency sensitivity (T1200499).

The preliminary design presented in this document builds on the LIGO and GEO experience with squeezing injection, two MIT table-top experiments (E1400404 and E1400406), and the development of an vacuum-compatible OPO at The ANU.

Tentative plans envision a possible squeezing upgrade to Advanced LIGO in 2017-2018, after a second long observing run O2.

While keeping this final target unchanged, **the main objective of the proposed design is to provide the option of delivering a squeezed light source to at least one of the two LIGO Observatories for an *early* squeezing implementation in 2016, possibly before the second observing run, O2.**

Early squeezing would not involve a filter cavity but would nevertheless require the following additions to Advanced LIGO:

- **HAM6**: a suspended, vacuum-compatible OPO; one suspended (tip-tilt) steering optic; readout of one RF frequency from the GW photodetectors in transmission of the OMC; high efficiency diodes for the OMC (already planned independent of squeezing effort);
- **HAM5**: modifications to the existing output Faraday to support squeezing injection (the open port is already present; it is facing the wrong side); one additional tip-tilt suspension for beam steering;
- **IN-AIR components**: a squeezer table which provides PUMP and CONTROL laser fields to the OPO; a breadboard on ISCT1 which provides a (fiber coupled) sample of the PSL beam to the in-air squeezed light table.

The early squeezing option seems particularly attractive for the LIGO Livingston Observatory:

- the likely vent of the vertex (G1500950) presents an opportunity to modify the HAM5 layout to accommodate steering optics for the squeezed beam;
- the poor measured isolation ratio of the current Output Faraday Isolator (15dB , see LLO log 19290) might require a swap of the output Faraday isolator; the new Faraday can be reconfigured for squeezing injection;
- swapping the current OMC diodes for high-efficiency units, already considered as a possible post-O1 activity, will reduce the loss in the readout path, a change clearly beneficial for squeezing;
- the swap of the OMC diodes, together with the replacement of the fast shutter that recently failed , will require an incursion in HAM6. Preparatory work for squeezed

light injection, such as the installation of a high quality window between HAM5 and HAM6 could be undertaken at this time;

- the vertex vent, together with the work required to fix the high-power oscillator in the PSL after the recent failure (see LLO log 18926) will result in several weeks of interferometer downtime; during which time, commissioning will not be possible and significant on-site person power can be dedicated to off-line preparation of the in-air squeezed light table and planning for squeezing installation.

3 Requirements

A squeezed light source for aLIGO must fulfil the following requirements:

Generation of high levels of squeezing ($> 15\,$dB produced by the OPO): this can be achieved by minimizing loss in the OPO cavity and OPO length noise (to minimize phase noise);

Isolation from back scattered light noise : spurious light from the interferometer anti-symmetric port reaches the OPO and is reflected back into the interferometer. Without scattered light control benefits from squeezing can be completely compromised;

Loss and phase noise control in the squeezed beam path : losses in the path between the OPO and the gravitational wave photo-detector must be minimized. Similarly, phase noise between the interferometer output beam and the squeezed beam must be as small as possible;

Long-term stability : the squeezed light source should be able to operate reliably 24/7, similar to all the other aLIGO subsystems.

A more detailed description of these requirements can be found in P1400064.

To mitigate the impact of radiation pressure noise at low frequency due to anti-squeezing, frequency dependent squeezing (with a filter cavity) needs to be injected in Advanced LIGO operating at full power (see P1300054). Since the current proposal targets aLIGO operations at low power, frequency independent squeezing (without a filter cavity) is still beneficial (see Appendix B).

4 Conceptual design for squeezing injection in Advanced LIGO

The conceptual design of the final Advanced LIGO squeezed light injection system presented in Figure 1.

An in-air table provides the PUMP and CONTROL laser beams, at 532 and 1064 nm, to an in-vacuum, suspended, optical parametric oscillator (VOPO).

The PUMP laser is phase-locked to the main interferometer laser by means of a sample of the PSL beam delivered to the in-air squeezer table using an optical fiber.

The squeezed beam is then routed via two tip-tilt suspended steering optics to the open port of the Output Faraday Isolator and injected into the interferometer. The beat between the interferometer output field and the squeezed field is then detected in transmission of the OMC and fed-back to the VOPO.

In its early configuration, this architecture is very similar to that adopted during the LIGO H1 squeezing test, albeit with two main differences:

- the OPO is not on the in-air table as before but it is suspended in-vacuum on the HAM6 platform;
- PUMP and CONTROL laser beams are fiber coupled to the VOPO.

In its final incarnation, when Advanced LIGO is operating at full power and limited by radiation pressure noise, the squeezed light source will incorporate a filter cavity to mitigate the impact of anti-squeezing at low frequency.

A 16-m, high-finesse cavity will be located between HAM5 and HAM4. The squeezed beam will reflect off this cavity before injection into the interferometer. By setting the filter cavity detuning to match the interferometer ponderomotive radiation pressure frequency, the impact of radiation pressure noise due to anti-squeezing can be suppressed.

Loss in the path of the squeezed beam from its source to the interferometer readout photodetectors allows regular vacuum to mix with squeezed vacuum, thus severely limiting the effectiveness of squeezing. Loss manifests itself primarily in imperfect optical components (for example Faraday isolator, OMC throughput) and mode mismatches (for example between the squeezed beam and the OMC). It is critical to minimize loss in order to guarantee high levels of measured squeezing.

An overview of the ongoing effort within the LIGO Scientific Collaboration to combat loss is summarized in T1400715, with a more detailed overview of plans for active wavefront control summarized in E1400426.

Most of the design choices presented in this document are guided by the experience gained in applying squeezing to LIGO and GEO. Several papers and technical notes motivating these decisions have been produced. A comprehensive list can be found in T1200499. Additional details can be found in P1400064 and references therein.

While the main choices will be explained in the following sections, a brief overview of the new features of the proposed Advanced LIGO design, as compared to the implementations in LIGO and GEO, follows:

Suspended, in-vacuum OPO cavity (VOPO) in GEO, and during the LIGO demonstration, the OPO is (was) located in-air on the squeezer table. There are several reasons why a similar approach would not be optimal for Advanced LIGO, primarily the stringent back-scattered light constraints, acoustic noise in the OPO cavity contributing to phase noise between the squeezed field and the interferometer output field and alignment stability;

Fiber coupling of pump and control laser beams to VOPO fiber coupling light to VOPO greatly simplifies in-vacuum optical layout and mode matching/alignment;

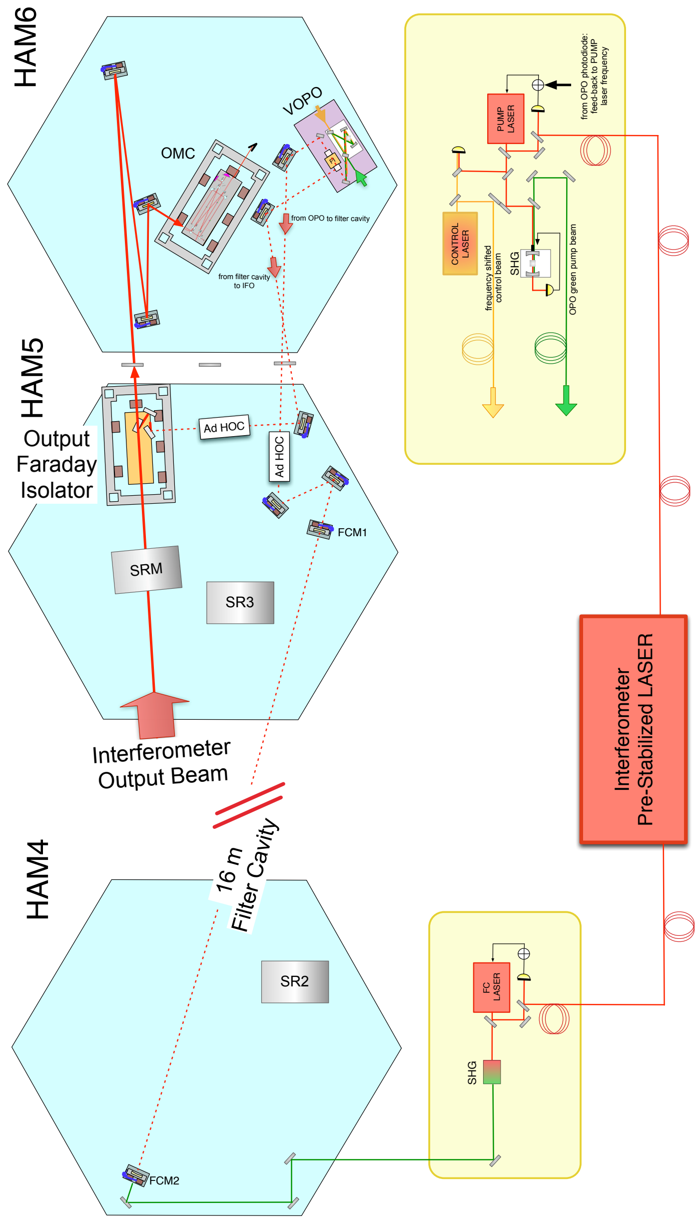

Figure 1: Conceptual design of the final squeezed light injection for Advanced LIGO . This should be considered as our vision for the final low-loss squeezed light injection system, including a filter cavity, i.e. **it is not the proposed layout for post-O1 installation.**

Control scheme in the original squeezing implementation at GEO, and in the LIGO experiment, a 1% pick-off before the OMC was used to sample the squeezed field and the interferometer field to generate an error signal for controlling their relative phase. GEO developed a better technique by extracting light in transmission of the OMC (P1200186). Moreover, GEO developed an alignment technique for the squeezed beam which allowed for higher and more stable levels of squeezing (P1500056). Also, the LIGO experiment highlighted some limitations of the technique implemented to lock the PUMP and CONTROL lasers to the PSL laser (see section 6). The proposed control scheme benefits from all of these fixes.

5 Overview of the in-Vacuum OPO (VOPO) design choices

5.1 VOPO cavity

The OPO proposed for Advanced LIGO is a bow-tie, doubly-resonant cavity, based on the ANU design (see P1000021) and is very similar to that employed during the LIGO H1 squeezing test. Two laser beams are delivered to VOPO: a green 532nm beam, which acts as pump for the OPO and a frequency shifted 1064 nm beam, which is the control field used to lock the squeezed beam to the interferometer beam. The OPO generates squeezed vacuum at 1064 nm by correlating the upper and lower quantum sidebands by means of a non-linear crystal.

A simplified diagram of the cavity is shown in figure 2.

The main components of the OPO are: input and output couplers, curved optics, a crystal and an oven.

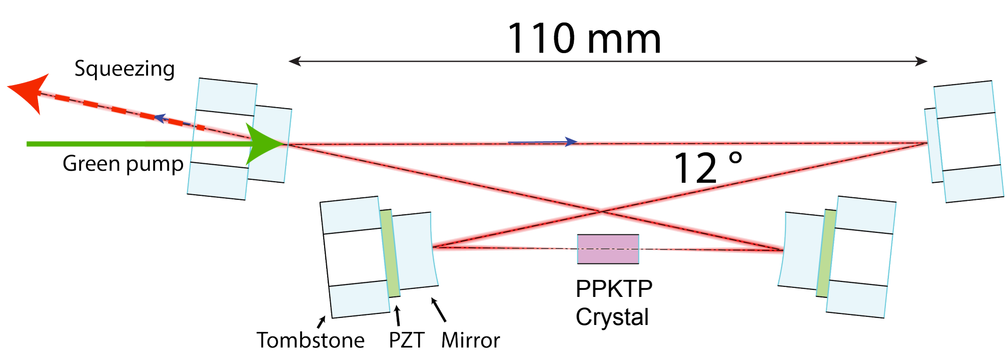

Figure 2: A diagram showing the OPO cavity design.

Several OPOs of this type have been operated in the last 10 years. High escape efficiency ($> 98\%$) has been measured in table-top experiments employing a doubly resonant, bow-tie OPO similar to the one proposed for Advanced LIGO (see for example measurements on the MIT glass unit [4]). High levels of squeezing (more than 10 dB down to 10 Hz) have also been measured in the past (see P1100202). A bow-tie configuration is particularly beneficial for Advanced LIGO as it intrinsically provides 40dB of isolation from back-scattered light (see P1200155).

While some of the optical parameters proposed for Advanced LIGO are different and the opto-mechanical layout has been adapted for in-vacuum operations, the main features of the OPO remain the same.

A detailed description of the aLIGO OPO optical design can be found in T1500465.

5.1.1 Non-linear crystal design

The medium responsible for the non-linear interaction in the OPO is a PPKTP crystal. The ANU design of the OPO relies on a **wedged** PPKTP crystal to achieve simultaneous resonance of the pump and fundamental frequencies, exploiting the different indices of refraction of PPKTP at 1064 nm and 532 nm. Dispersion compensation is achieved through translation of the crystal transverse to the beam propagation direction, which produces variations in the optical path length experienced by the two beams. The phase-matching temperature is around $30° - 35°$.

Details of the crystal parameters and dispersion compensation tuning can be found in T1500350 and references therein.

5.2 VOPO fibers and feed-through

Optical fibers are used to deliver the pump green light and the control laser 1064 nm light to the VOPO. Because of UHV compatibility, extensive research and testing has been carried out in the last year to find suitable vendors.

A summary can be found in T1500417.

5.3 VOPO oven

An oven is needed to maintain the crystal at its phase matching temperature. ANU designed and built an oven for in-vacuum operations (see D1500020). Tests at ANU identified a limitation of the original design – the lack of a translation stage for the crystal limited in-vacuum performance due to a shift in the optimal operating point relative to in-air operation (see P1500095). At MIT we have therefore constructed a remotely controllable translation stage for the crystal. This oven is currently under test. At the same time, we are investigating options for optimizing the current design in order to reduce the thermal load.

5.4 VOPO assembly

The OPO cavity adopted during the H1 squeezing experiment was built by mounting super polished 0.5" optics on regular opto-mechanical mirror mounts (see figure 3, left side). For in-vacuum operations, ANU prototyped a monolithic glass OPO (see P1500095), similar in concept to the aLIGO Output Mode Cleaner, which guarantees low length noise and thermal stability.

ANU built the cavity by using optical contacting (see G1500364), which has the advantage of being reversible, and therefore particularly suitable for experimenting assembly procedures.

Components to build a second cavity, similar to the ANU one, were shipped to MIT, where a second glass OPO was built. An unfortunate choice of the cavity length required to de-contact several optical components (MIT log Jun 29) and that turned out to be difficult.

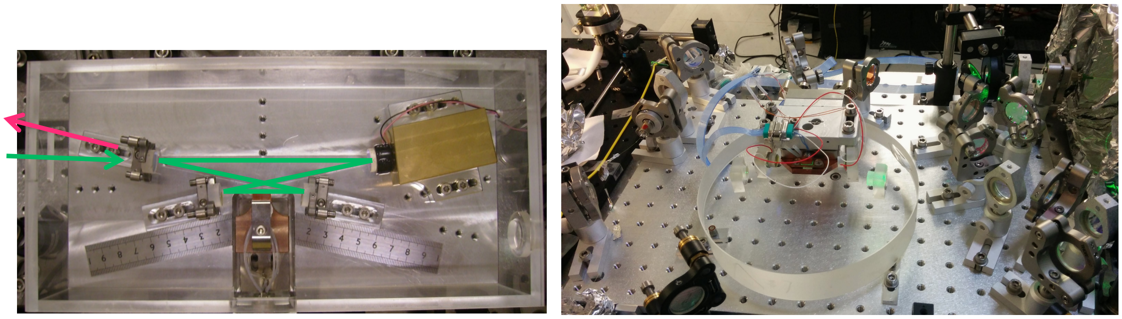

Figure 3: OPO cavity built with opto-mechanical components, as adopted during the H1 squeezing experiment for in-air operations(right); monolithic glass OPO cavity, built for in-vacuum operations, currently under test at MIT (left).

While a monolithic glass cavity has several advantages, they seem to come at the expense of a complicated and time consuming assembly procedure.

While succeeding in building a cavity, and proceeding with testing, we therefore decided to build a cavity using opto-mechanical components, more similar to the original in-air OPO.

5.5 VOPO suspension

A single stage suspension is sufficient to reduce back scattered noise below requirements. After investigating the option of adopting the design of the double stage OMC suspension, we decided to re-design a single stage suspended platform. A preliminary design is described in E1500383.

6 Advanced LIGO squeezing control scheme

The control scheme proposed for Advanced LIGO is conceptually similar to the one implemented during the H1 squeezing experiment.

Two laser beams are delivered to VOPO: a green beam, which acts as pump for the OPO and a frequency shifted 1064 nm beam (CLF), which is the control field used to lock the squeezed beam to the interferometer beam. These two beams are fiber coupled from an in-air table. The green beam is produced by passing a 1064 nm laser beam (PUMP) through a resonant Second Harmonic Generator (SHG); the control field is produced by phase-locking an auxiliary CONTROL laser to the PUMP laser, and frequency shifting it with respect to the PUMP carrier frequency.

The servo design of the H1 squeezer experiment was guided by the desire to have a high bandwidth feedback from the anti-symmetric port detector measuring the SQZ angle to the laser frequency of the pump laser. This allows for maximum suppression of path length fluctuations between the interferometer field and the squeezer field. The bandwidth was ultimately limited to about 10 kHz by the free-spectral-range of the arm cavities. By moving the OPO in vacuum it is possible to use its length as a stable reference and lock the squeezed beam with a much lower bandwidth to the interferometer. The new servo design locks both the pump and controls lasers with a high bandwidth to the OPO and then uses the OPO length as a frequency actuator to match the squeezer field to the interferometer field. This is shown in Fig. 4.

We also propose to use a VCO to set the frequency of the controls sideband. The H1 experiment started out with fixed frequency oscillators for both phase locked loops (PLL), but the pump laser setup was later changed to use a VCO as a frequency actuator. This yielded a much improved actuator range and replaced an actuator comprised of a lower bandwidth PZT and an additive offset into the PLL error point for faster response. This configuration worked very well and for the Advanced LIGO squeezer we propose to copy this scheme to the controls laser, eliminating its PZT and additive offset actuator pair. This will allow for a simpler feedback design with a higher range and the elimination of the in-house PZT actuator design.

6.1 Choice of control field frequency

A critical parameter of the squeezing control scheme is the choice of the frequency offset between the control laser and the pump laser.

There are a number of considerations we have thought of:

- filter cavity resonances (TEM00 and other modes)
- arm cavity FSR (which limits CLF loop bandwidth)
- SRC + arm cavity behavior (i.e., near SRC resonance, or near anti-resonance?)
- SRC length noise, which makes phase noise (dependent on #3)
- OMC length noise (which induces phase noise)
- OMC line width (which determines CLF transmission)
- OPO length noise (which induces phase noise)
- technical noise coupling (e.g., CLF intensity noise)
- RF electronics (generally favoring frequencies $5 - 50$ MHz)
- DC PD electronics (possibly favoring frequencies below a few MHz)
- WFS electronics (readout with beat against SI45MHz sidebands)

By "phase noise" we mean "a difference in the phase of the CLF and the squeezed field, as readout with the carrier".

The arm-cavity resonances have historically been avoided by the CLF, since phase locking loop derived from the CLF is limited in bandwidth by the phase shift on reflection from

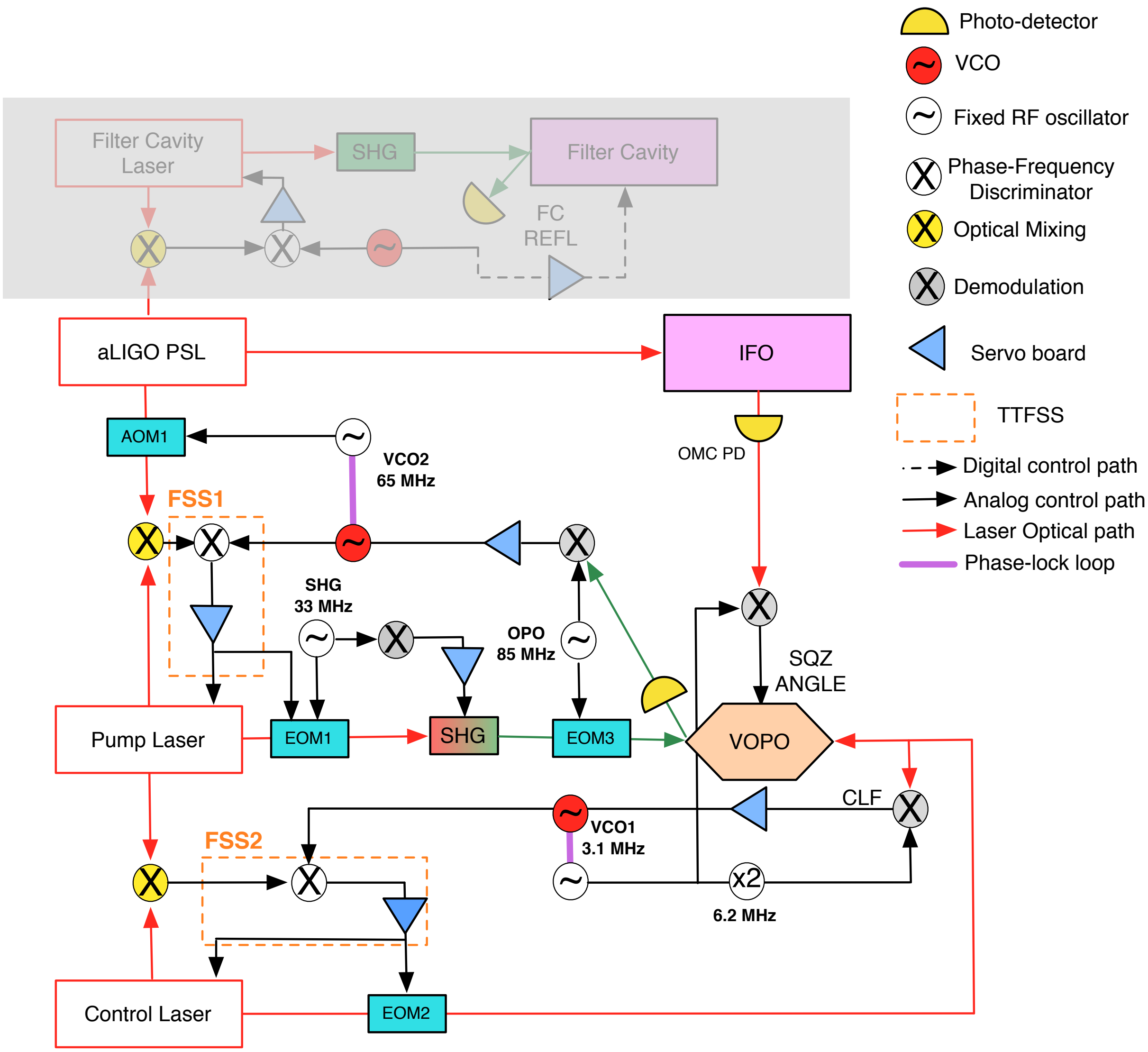

Figure 4: Block diagram of the squeezer control scheme. The grey area represents the control scheme for the filter cavity.

the interferometer. This appears to limit the bandwidth of this loop to at most 16 kHz for aLIGO, assuming the CLF is placed near an arm cavity anti-resonances (ACAR).

The filter cavity (FC) resonances are "easy to miss" since the FC has a very narrow line width. In any case, some care should be taken to choose an ACAR which does not have an FC resonance within 20 kHz. Clearly good mode-matching will be required, so we needn't consider a large number of higher-order-modes.

Signal recycling cavity (SRC), output mode cleaner (OMC) and optical parametric oscillator (OPO) cavities all have the effect of converting length noise into a difference between CLF and carrier phase. This is a fundamental non-ideality in the CLF strategy which cannot be avoided when highly dispersive elements (e.g., resonant cavities) are present in the optical system. In all cases, the damage can be minimized by keeping the length noise of the cavity small compared to 0.1% of the cavity line width:

$$\Delta\phi \simeq 2\pi\mathcal{F}\,\frac{\Delta z}{\lambda} \ll 10^{-3} \tag{1}$$

In the case of the OPO, the CLF frequency can be kept within the cavity line width ($\simeq$ 15 MHz), such that the squeezed field and the CLF acquire similar phase shifts. For the SRC and OMC this is not possible, so the length noise must be kept below 10 pm and 1 pm respectively.

For OMC residual length noise, measurements performed by Koji Arai estimate between 0.01-0.1 pm rms (LHO log entry 18034). While looking at current SRCL error signal residuals gives 10 pm RMS, mostly dominated by $1-3$ Hz motion.

Technical noises on the CLF are generally intensity or frequency noise which produces noise sidebands at the CLF-carrier difference frequency. These noise sidebands, if above shot noise, will contaminate DARM. This consideration, along with the general easy of RF electronics design, pushes us to avoid frequencies below 1 MHz.

To derive signals from the OMC reflection wavefront sensors (WFS) as has been done in GEO600, we will need to demodulate at the beat frequency between the CLF and the 45 MHz sidebands. Keeping the CLF frequency below 10 MHz will probably make this an easy retuning of existing WFS.

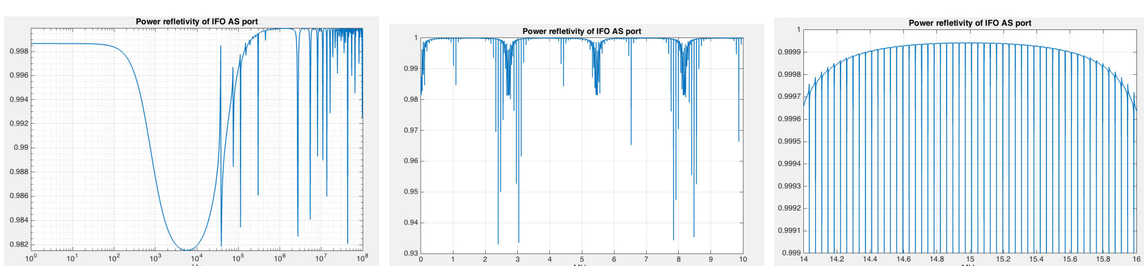

Figure 5: Interferometer reflectivity, from AS port The dominant structure comes from the signal recycling cavity (56 m long, 2.68 MHz FSR). The fine structure with 37 kHz width are the arm cavity resonances.

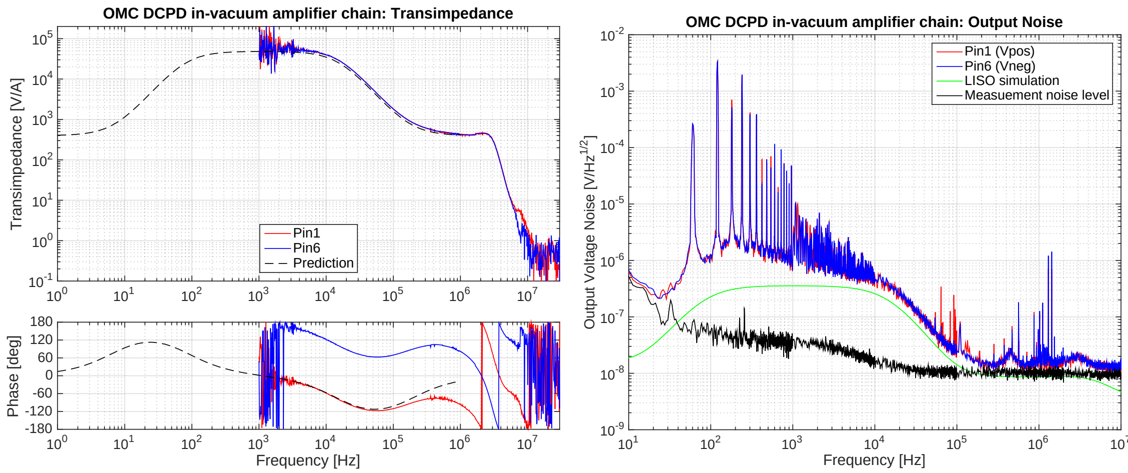

Figure 6: **OMC DCPD** The response, including whitening filters, cuts off at 3 MHz. See Koji Arai's log entry for more information about the measurement.

All of these factors point to a low CLF frequency near an SRC anti-resonance; the first 2 are 1.3 MHz or 4.0 MHz. The lower of these at 1.3 MHz is disfavored by the presence of laser technical noises below 2 MHz, making 4 MHz a better choice. Unfortunately, the response of the currently installed DCPDs drops quickly above 3.0 MHz (see 6), so that there is some incentive to reduce the CLF frequency (see appendix A) The width of the SRC resonance is such that at 400 kHz away from the resonance is almost as good as the anti-resonance (which itself is a soft requirement), such that a CLF of 3.1 MHz seems a good choice given the limitations of the DCPDs.

In case the OMC PDs readout chain is re-designed, then a higher CLF frequency could be considered.

7 Overview of squeezing sub-system (SQZ)

Figure 7 shows a block diagram of the SQZ subsystem, and Figure 8 shows an overview of the HAM5 and HAM6 proposed layouts.

The DCC tree collecting all the documents related to the squeezing sub-system can be found at E1500358. It comprises:

System overview: E1500359

Opto-mechanical layouts: E1500360, including HAM5 and HAM6 layouts, the in-air squeezing table layout, and the proposed modifications to ISCT1 for sampling the PSL light;

VOPO: E1500361; this node collects documents and drawings for the VOPO cavity, the suspended platform with the routing optics to the VOPO cavity, fiber choices, VOPO suspension;

Electronics&Automation: E1500362.

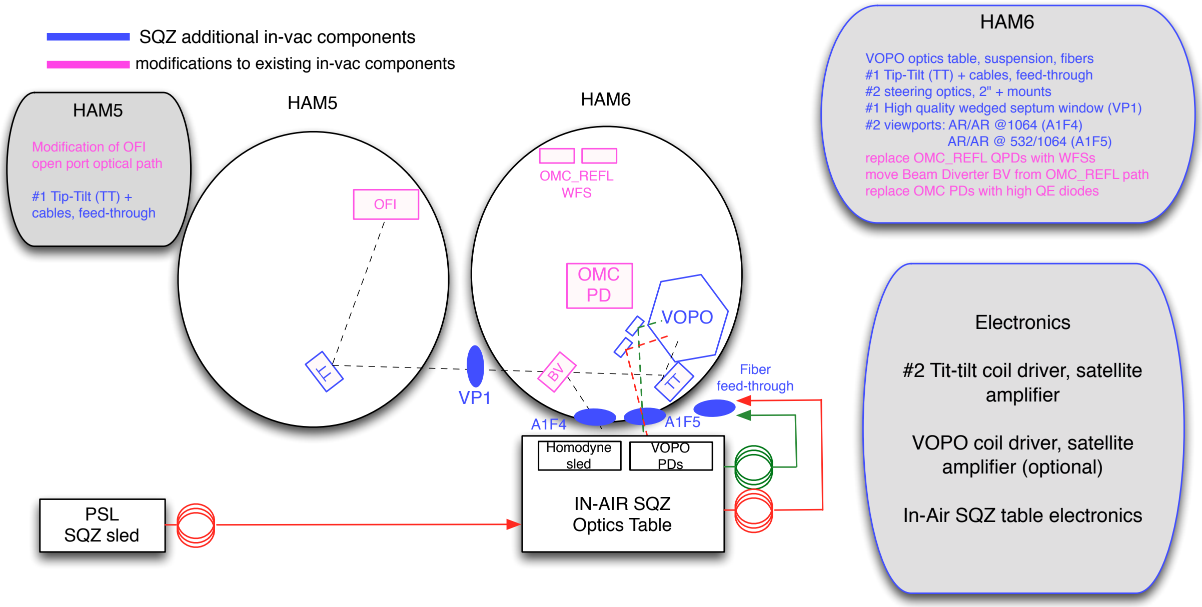

Figure 7: Block diagram of the squeezing subsystem SQZ.

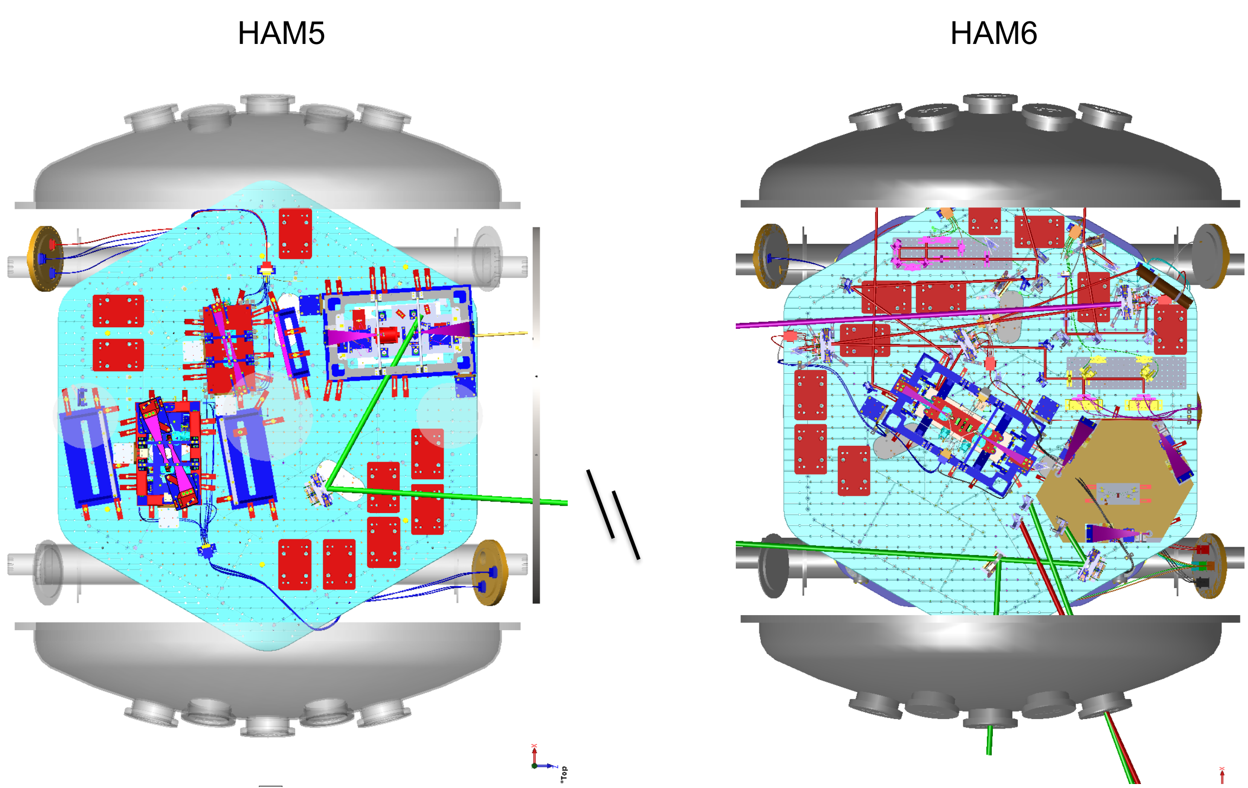

Figure 8: View of the HAM5 and HAM6 chambers with SQZ components.

8 System interface: modifications/additional in-vacuum components

8.1 VOPO in HAM6

The VOPO will be installed in HAM6, on the side currently unoccupied by ISC components.

The installation of the VOPO suspended platform in HAM6 will require a rebalancing of the HAM6 table. This is not expected to be a problem; current balancing masses will be repositioned.

8.2 Squeezed beam path from the VOPO to the Faraday

In order to steer the squeezed beam from VOPO (in HAM6) to the OFI open port (HAM5) we will use two tip-tilt style suspensions with flat optics.

One tip-tilt will be placed in HAM5, and one in HAM6. No modification of the existing optical layout for the main interferometer beam will be necessary.

The mode matching telescope for the squeezed beam will be built on the VOPO suspended platform. The lens solution shown in figure 9 places one lens before the squeeze-faraday, and one after the faraday, with 21" between them. Moving either lenses in this solution has essentially the same effect on the output beam shape. A displacement of 2 cm from the optimal position decreases the overlap with the target by 9%. Moving both lenses differentially decreases the overlap by 24%, while moving them both in the same direction changes the overlap by 0.7%. If possible, both lenses should be located on translation stages capable of moving a few cm (e.g., PI Q-521,330). Having 2 actuators will double the range of the differential actuation, and allow for some exploration and fine tuning of the common degree of freedom.

A more complex lens solution which allows for sensitive control of both beam size and waist position may be possible, but it would introduce more optical elements, thereby increasing loss and complexity.

A beam diverter will be placed in the path of the squeezed beam to HAM5, in order to be able to send the squeezed beam to the homodyne detector on the in-air squeezer table for diagnostic.

One option could be to re-locate the beam diverter currently located in the OMC_REFL path, as the in-ar OMC REFL diodes are not actually used.

Note that 27 tip-tilts are currently present at both sites (see ICS records. Only 5 are currently used in each detector. There are therefore 12 tip-tilts already available (the actual assembly status need to be checked).

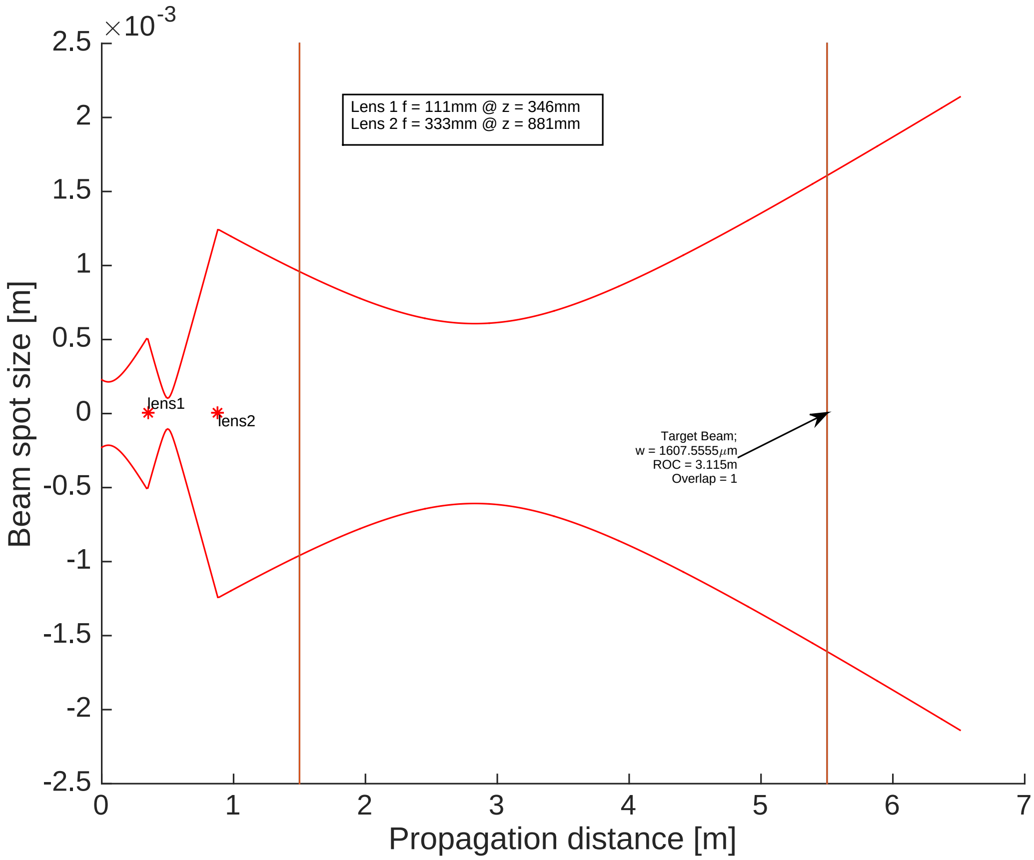

Figure 9: Mode matching solution for the squeezed beam leaving the OPO.

8.3 Output Faraday Isolator modifications

A view of the Faraday table is shown in Figure 10

The aLIGO Output Faraday Isolator (OFI, D0900623) was already designed with the idea the Faraday could be used for squeezing injection. For this reason, a thin film polarizer (horizontal transmission, vertical rejection) is used to create a low loss open port, before the second calcite polarizer. Two posts for holders were placed in front of the thin film polarizer for possible steering optics for the squeezed beam.

When the aLIGO OFI was installed, a beam dump was placed in front of the thin film polarizer (see figure 10), and no optics holder were installed for the steering optics. The original design of the OFI somehow assumed that the squeezed beam would be injected from an in-air table adjacent to HAM5, on the north side. In the proposed layout, the squeezed beam is routed to the Faraday from the opposite side.

Figure 10 shows one possible solution to accommodate squeezed light injection by minimizing changes to the current OFI: the wave plate can be moved by 0.5mm toward the rotator, while one of the locations originally set-up for squeezed light steering optics can be used to send the squeezed beam toward the center of HAM5, where it will be caught by a steering optic suspended by a tip-tilt.

This approach won't require modifications to the current OFI sled. The only additional components will be a 1" optic with optic holder, and two dog clamps to relocate the wave plate.

8.4 Wave-front sensors for squeezed beam alignment

The alignment of the squeezed beam with respect to the interferometer beam can be controlled by using WFSs in reflection to the OMC.

This scheme, developed in GEO600, works by beating the CLF field with one of the interferometer sideband, which is used as local oscillator.

Currently, two unused QPDs are located in reflection to the OMC. By using the interferometer 45 MHz sideband as local oscillator, regular aLIGO WFSs, tuned for 36 and 45 MHz, could be easily retuned to for 42 MHz.

8.5 High quality AR/AR septum window for HAM6

Figure 11 shows the viewports location and naming convention of the output septum plate in HAM6. The interferometer output beam is transmitted through viewport VP3, that is the only septum viewport currently used. VP1 and VP2 are covered by a viewport septum blank D1101718. In the SQZ layout we envision, the squeezed beam will be routed from HAM6 to HAM5 through VP1. VP1 needs therefore to be equipped with a AR/AR high quality, wedged viewport as VP3.

The D1101718 viewport blank needs therefore to be replaced by a Septum Viewport Assembly D1101092.

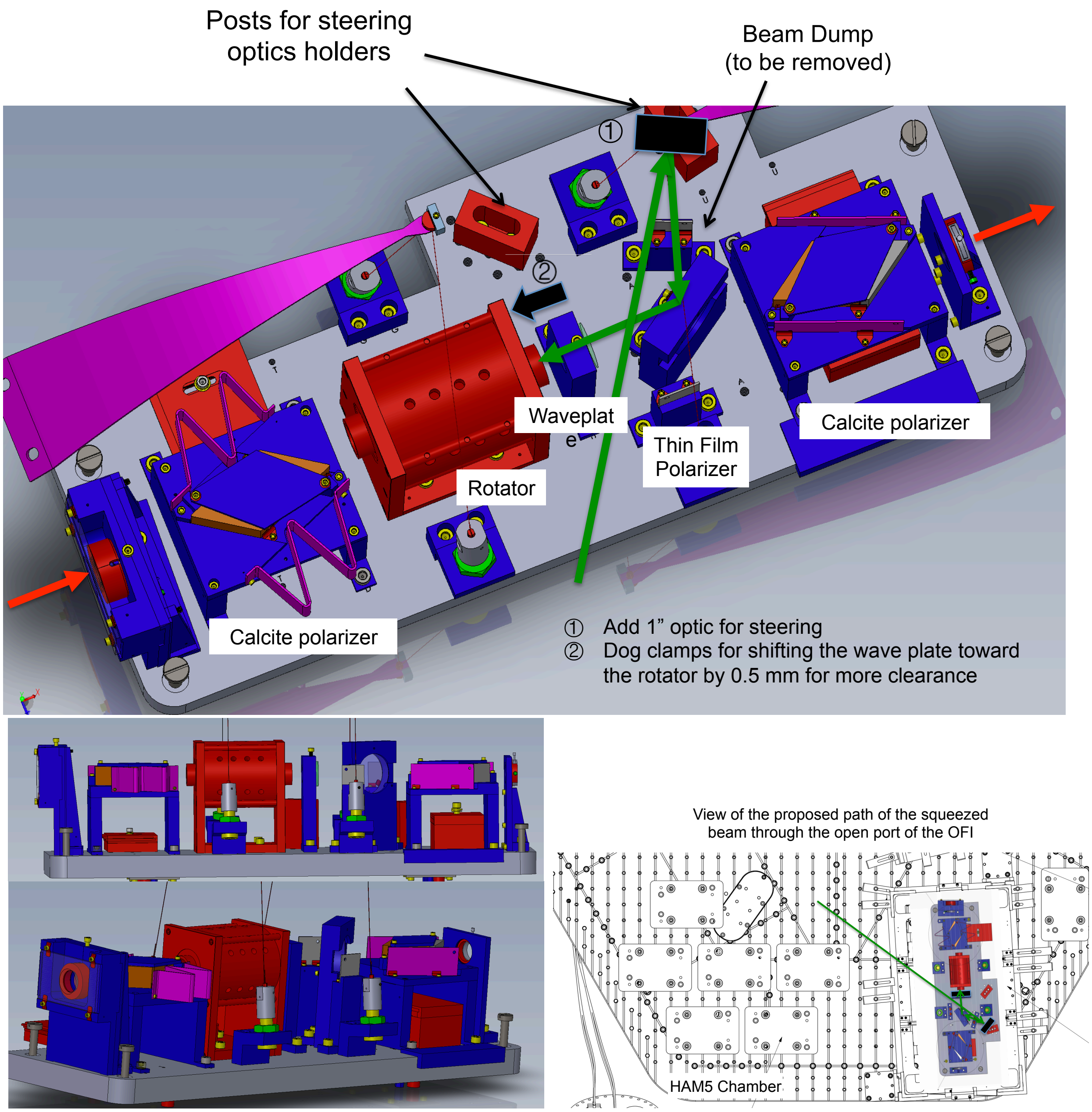

Figure 10: Overview of the aLIGO Faraday and modifications needed to allow for squeezed light injection.

In particular, it requires:

- a high quality wedged 6" viewport D1101005; according to ICS, 11 of this type of windows are currently in storage; they do not appear to be clean;
- septum viewport flange D1101117; according to ICS, at least 5 of this type of flanges are already cleaned and baked in storage;
- high quality, 6in Viewport Clamp, wedged D1101115; according to ICS, at least 9 of this type of flanges are already cleaned and baked in storage.

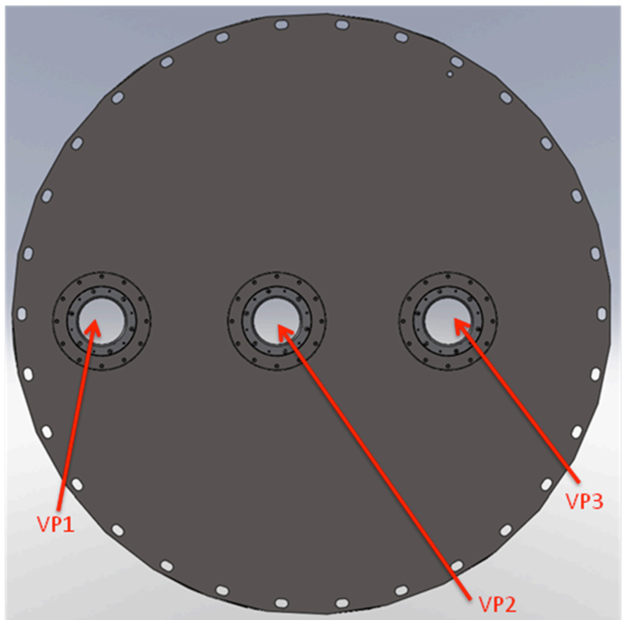

Figure 11: Naming convention and location of the viewport in the HAM6 septum, as seen from HAM6. The interferometer beam leaving the Output Faraday reaches HAM6 through the VP3 window.

8.6 High quality AR/AR windows for HAM6

Two high quality windows are necessary for HAM6: one for the squeezed beam (AR/AR@1064nm) and one for the OPO and CLF reflected signals (AR/AR@1064+532nm).

9 System interface: modifications/additional in-air components

9.1 In-air squeezer table

The in-air squeezer table will be positioned in the LVEA next to HAM6, on the South side (the opposite side with respect to the ISCT6 table).

The alternative will be to locate the table on the East side. While more space would be available in that area, currently vacuum pumps are located on one of the flanges on that side. Moreover, the in-vacuum optical layout makes the South side preferable.

A 3' deep table will allow clearance between the table and the corridor wall, similarly to the case of the IOHT2R table next to HAM2.

A 3' x 8' table will be able to accommodate all the required components (see D1500297).

Figure 12: View of the South side of HAM6 (left) and the East side (right). The ISCT6 table is located on the North side.

9.2 Sled for sampling PSL light in ISCT1

A sled to fiber couple PSL light to the in-air squeezer table will be placed in ISCT1 (see D1500298). No major modification of the existing set-up will be necessary.

10 Plausible path for "early" squeezing (post-O1)

The main goal of this proposal is to have the option of injecting squeezing light in aLIGO sometime next year.

At this time, it seems that LLO offers several favorable conditions for squeezing, in terms of status of the detector and available person power. Considering that the LIGO H1 squeezing experiment has been carried on at LHO, and LHO staff has already experience with squeezing, it seems that starting the process for squeezing at LLO is a good opportunity to create local expertise. Without attempting to predict the course of commissioning activities and upgrades post-O1 at both sites, we suggest to perform the actions:

- carry forward the engineering and optical work required to modify the current layout of OFI, so that a new OFI can be installed at the time of the vertex vent. Because of the poor L1 OFI isolation, it seems that this work could be coupled with additional isolation measurement on the new unit. Also, Koji Arai is currently performing a set of measurements to investigate loss in the OFI components (see Caltech log 243 and Caltech log 241). Some of the finding of his work could in principle be incorporated;

- at the time of the vertex vent, install the tip-tilts (at least the one in HAM5), and perform the septum and high quality windows modifications;
- tune two aLIGO ASF WFS for 42 MHz.

At the same time, in order to prepare the in-air components, we will need:

- funds for starting procurements on long lead items (such as custom optics and electronics)
- allocation of on-site person power for procurements and testing of the electronics needed to operate the squeezer, and design of the squeezer table enclosure and feed-throughs.

Once the final design of the VOPO is completed at MIT (see R&D program T1500488), a VOPO unit could be built, shipped to the site and installed in HAM6, without requiring an additional vent of the vertex.

An alignment procedure involving an auxiliary laser source can be developed to pre-align the HAM5 components in the squeezed beam path; fiducials can be installed in HAM6 at the time of the vertex vent as reference.

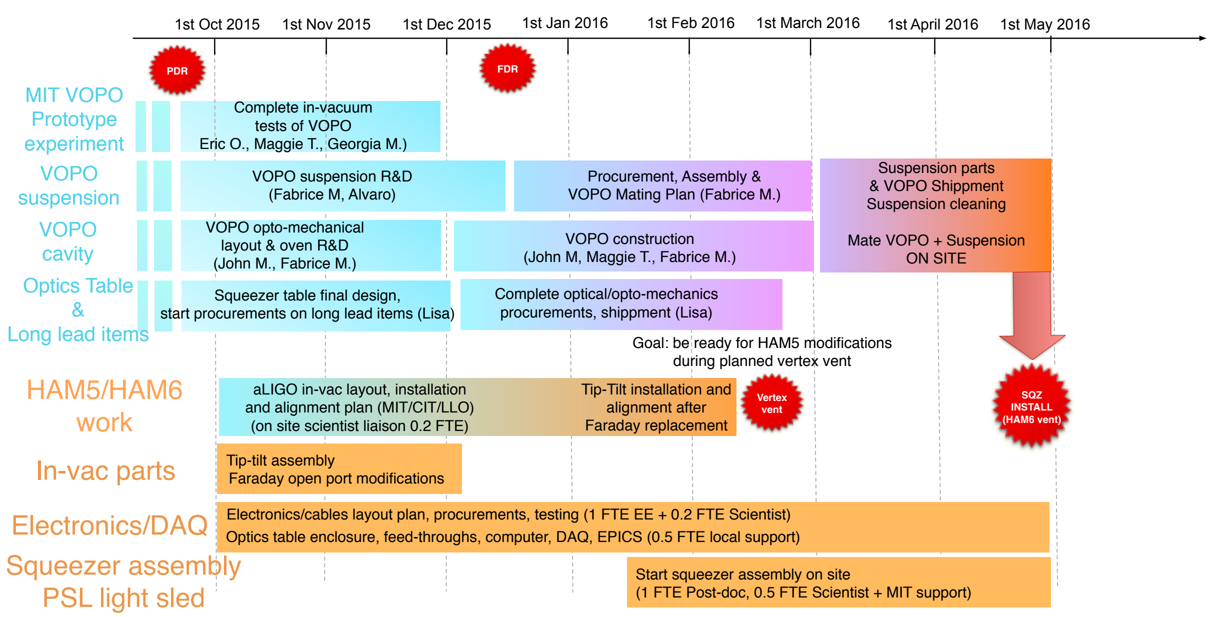

Figure 13: Tentative timeline for squeezing post-O1.

A Choice of CLF frequency for squeezing angle control

A.1 Sensor noise

We estimate the sensor noise in the error signal used to control the squeezed field angle relative to the interferometer field, obtained in transmission to the OMC.

The size of the error signal is quadrature dependent; by choosing the worse case scenario:

$$\text{Error signal (watts/radian)} = 2 * \sqrt{\mathrm{P_{DC}}} * \sqrt{\mathrm{P_+}} - \sqrt{\mathrm{P_-}} = 1.27\text{x}10^{-4}\ \text{W/rad} \tag{2}$$

where P_{DC} is the power on the OMC PDs ($P_{DC} = 20$ mW), P_+ is the upper CLF sideband ($P_+ = 0.595$ uW), P_- is the generated CLF sideband ($P_- = 0.105$ uW).

As a requirement, let's assume that we want the sensor noise to contribute less than 1 mrad RMS over a 10kHz bandwidth, therefore:

$$\text{sensor noise} < 1.27\ \text{nW}/\sqrt{\text{Hz}}\ \text{at4.1MHz} \tag{3}$$

In terms of the output referred noise, and given a measured transimpedance of 60 V/A at 4.1 MHz (see Figure 6) the sensor noise requirement is:

$$\text{sensornoise} < 1.27\ \text{nW}/\sqrt{\text{Hz}} \times 0.7\ \text{(A/W)} \times 60\ \text{(V/A)} = 53\ \text{nV}/\sqrt{\text{Hz}} \tag{4}$$

The actual sensor noise at 4.1 MHz is $20nV/\sqrt{(}Hz)$, less than a factor of 3 below.

The transimpedance at 3 MHz is 5 times higher (300 (V/A)), those relaxing the requirements.

A.2 Intensity noise of the CLF field in transmission to the OMC

We estimate the classical intensity noise of the CLF field after the OMC relative to its shot noise.

The intensity noise of CLF field at its origin is assumed to match that of a typical NPRO. We take our estimate from the RIN specification given in the Lightwave 126 manual. This estimate is plotted in Figure 14. We convert these RIN values into W/$\sqrt{\text{Hz}}$ as follows

$$\widetilde{dP}_{\text{intensity}} = \sqrt{2P_{\text{dc}}^2 10^{\text{RIN}/10}}, \tag{5}$$

where P_{dc} is the dc CLF power after the OMC. The shot noise, in identical units, at the same location, is estimated according to

$$\widetilde{dP}_{\text{shot}} = \sqrt{2P_{\text{dc}} h f_{\text{laser}}}, \tag{6}$$

P_{dc} may be calculated as follows

$$P_{\text{dc}} = P_{\text{inc}} T_{\text{OPO}}(f) G T_{\text{IFO}} T_{\text{OMC}}(f), \tag{7}$$

where $T_{\text{X}}(f)$ is the frequency-dependent transmissivity of a cavity X (see Figure 15) and the remaining parameters are as defined in Table 1.

The ratio $\widetilde{dP}_{\text{intensity}}/\widetilde{dP}_{\text{shot}}$ is plotted in Figure 16.

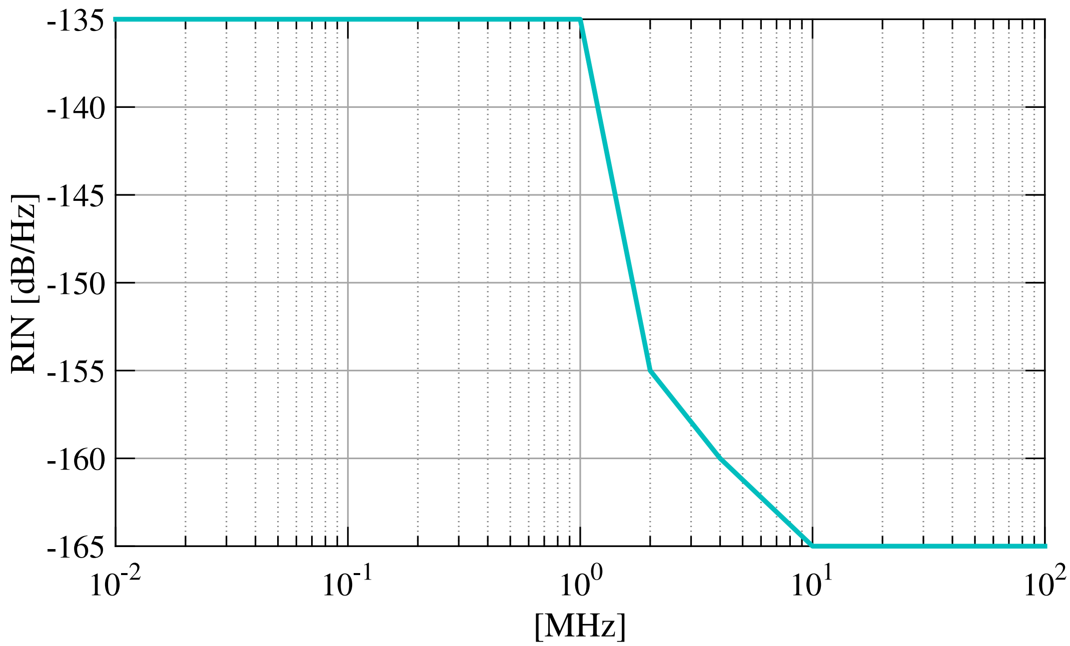

Figure 14: RIN estimate for CLF field before OPO. These values are based on those of a Lightwave 126 laser with the noise eater engaged.

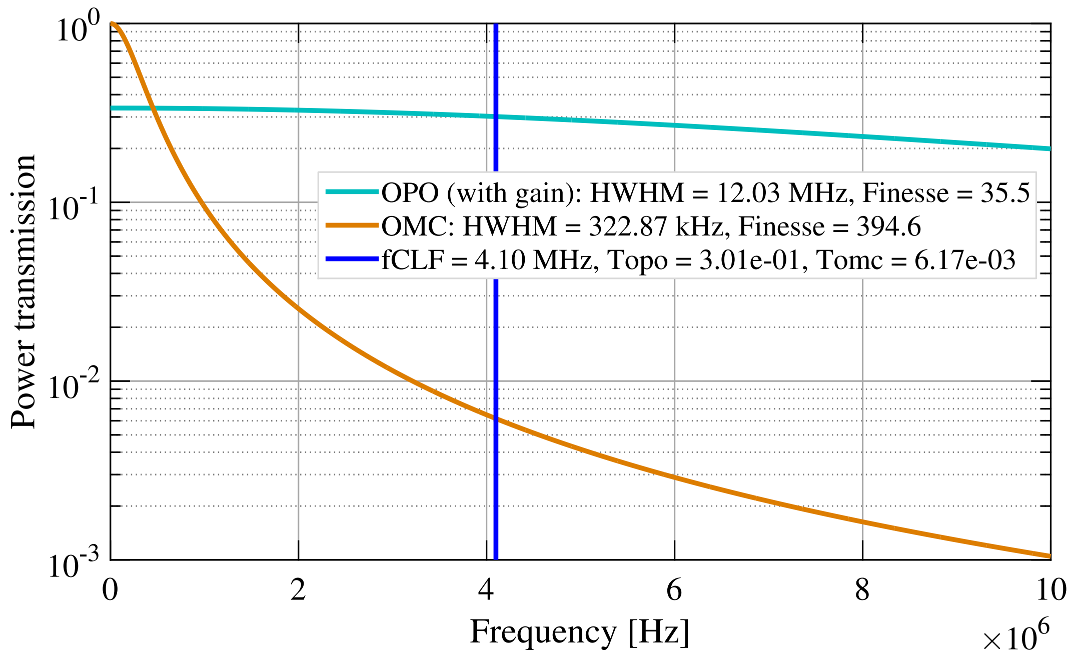

Figure 15: Power transmission of the OPO and OMC cavities as a function of CLF frequency. OPO values include a nonlinear gain of 10.

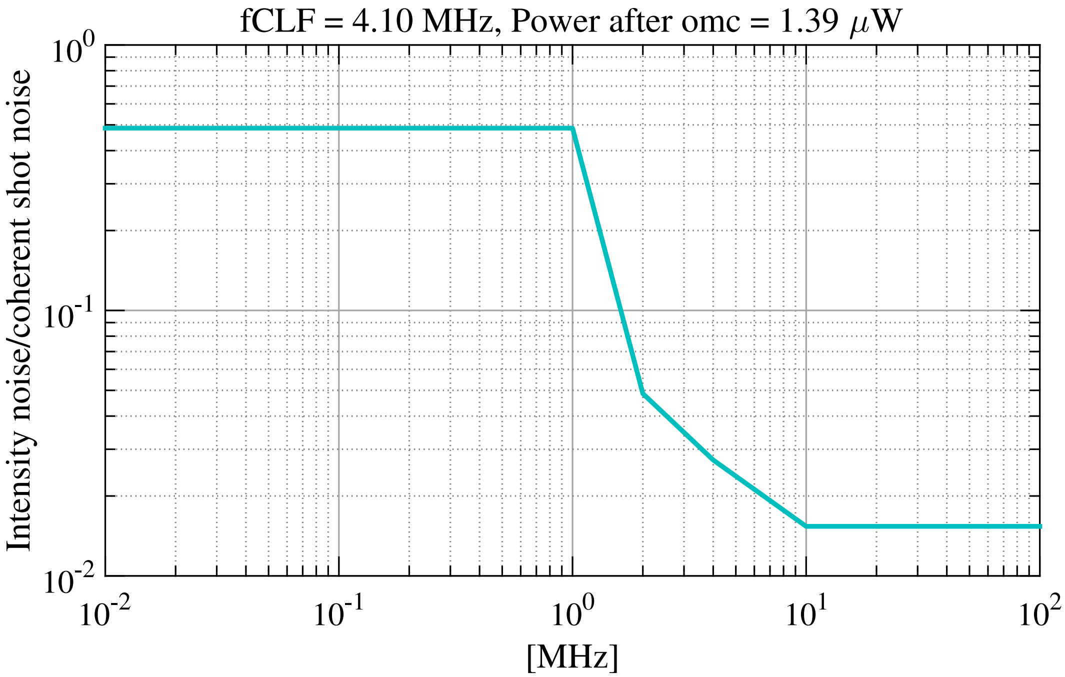

Figure 16: Ratio of intensity noise to shot noise in the CLF field after the OMC.

Table 1: Parameters used in determining the classical intensity noise and shot noise in the CLF field after the OMC

Parameter	Symbol	Value
CLF power incident on OPO	P_{inc}	1 mW
Parametric gain of the OPO	G	10
FWHM linewidth of the OPO	-	18.345 MHz
FWHM linewidth of the OMC	-	646 kHz
Power transmission of the IFO	T_{IFO}	0.75

B Prediction for squeezing impact in L1 post-O1

Range calculations are based on the latest GWINC version which accounts for redshift correction (GWINC revision 2677). The L1 reference curve used in these calculations is the one measured on March 1st, 2015, which, according to the latest int73 GWINC code, corresponds to 69 Mpc. Note that this L1 sensitivity has been measured with an abnormally high gas noise; for this reason, a model of the predicted gas and squeeze film damping noise with the additional 2 pumps (implemented in July 2015) are used to make a more realistic prediction.

B.1 Analysis of the L1 sensitivity

Theoretical curve based on GWINC, given the high gas noise of March 2015, predicts 95 Mpc (see figure 17).

Of the "missing" 26 Mpc:

- 14 come from the "unknown" allegedly $\frac{1}{f^{3/2}}$ broadband noise which limits the sensitivity in the bucket (95 Mpc $\rightarrow$ 81 Mpc);
- 9 Mpc comes from the scattering peaks above 50 Hz (81 Mpc $\rightarrow$ 72 Mpc)
- the remaining 3 Mpc come from excess noise below 50 Hz.

The point here is just to say that, as it is well known, even with high gas noise and low power, reducing scattered noise and the broadband noise in the bucket would be enough to reach more than 90 Mpc.

Figure 25 shows what is the theoretical expected sensitivity for O1, given the recent improvement of gas noise with 2 extra pumps (based on Ryan's calculations). The maximum possible range is increased to 129 Mpc.

C Comparison of power increase vs squeezing post O1

Here we assume that the OMC diodes will be replaced after O1 with high quantum efficiency one, and readout loss will be reduced by 10%. Also, in this case low gas with all new pumps is assumed ("worst case" for squeezing); higher squeeze damping noise minimizes drawbacks from squeezing, so this case is not considered here.

Figures 20 21 22 show that the disadvantages of 25W + 3 dB SQZ compared to 50 W + no SQZ are minimal. Also, injecting 3 dB of squeezing at 50 W still improves the range, up to a maximum of 180 Mpc.

C.1 Scenario with the extra "thermal" noise in the bucket, scattered light fixed

Even assuming that the currently "unknown" $\frac{1}{f^{3/2}}$ noise in the bucket is not fixed, the predicted sensitivity given the current gas noise (with the 2 additional pumps) is 103 Mpc.

The impact of 3dB of squeezing in this scenario would be +15% (see figure 24); since squeeze damping noise is still high, squeezing is equivalent to increase the power to 50W.

Further improving the gas noise with all new pumps would not help much if adopting squeezing.

Replacing all the pumps with new pumps will further improve the maximum possible range to 138 Mpc (figure 19).

C.2 Pessimistic scenario with scattered light and excess thermal noise not fixed

Here we assume that we are not able to improve scattered light noise, and we can't find the source of the the broadband noise in the bucket. The only noise sources that we improve are quantum noise and gas noise. Here we assume that the OMC diodes have been replaced.

In this case the low frequency noise is high, and the impact of anti-squeezing is negligible (see figure 26).

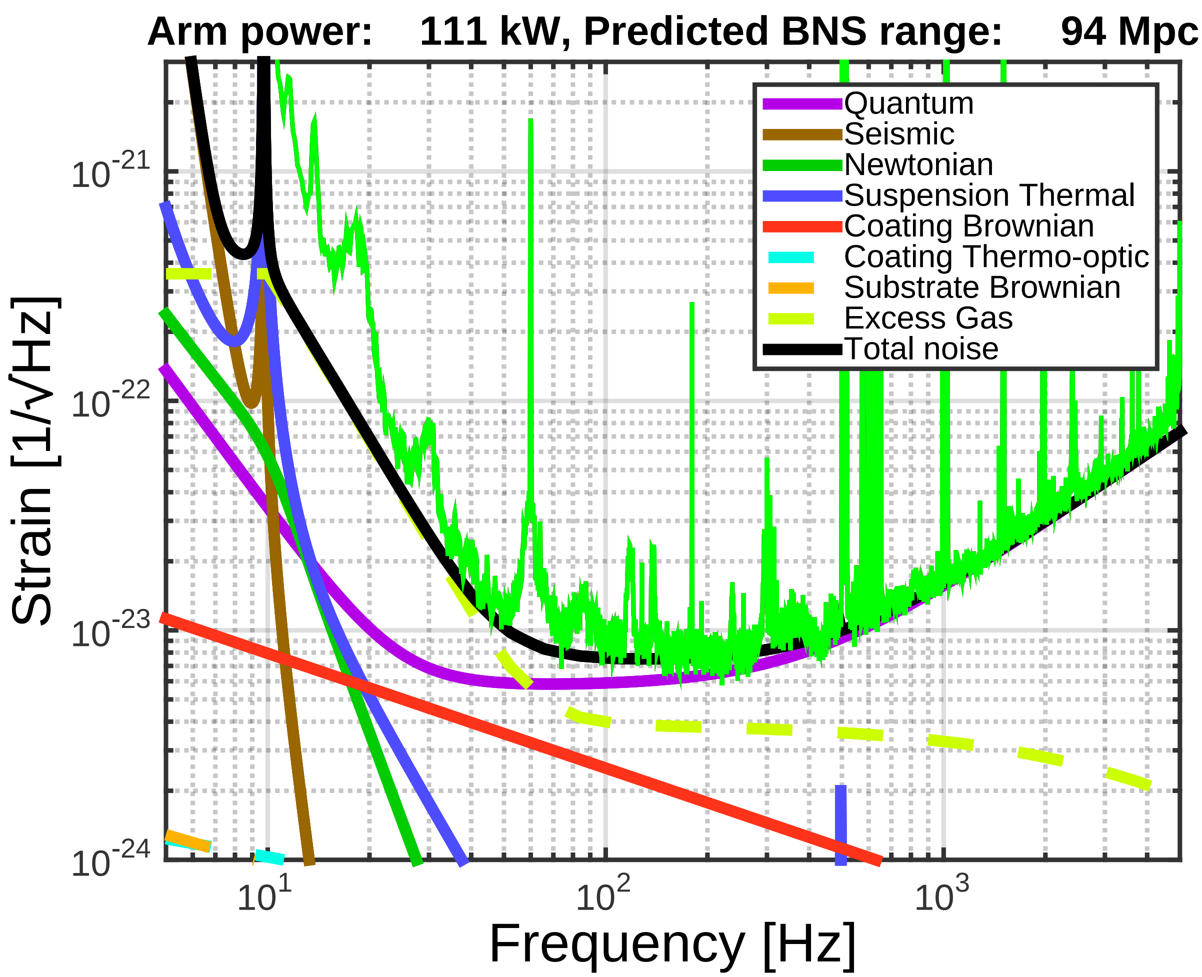

Figure 17: $\mathbf{25W,\ June2015\ gas}$. L1 sensitivity (March 1st, 2015 - 69 Mpc according to current int73 GWINC code), compared with the prediction based on fundamental noises calculated with GWINC (95 Mpc). As explained in LLO log entry 18530, the discrepancy can not be accounted for based on the current understanding of the noise budget. An unknown source with slope $\frac{1}{f^{3/2}}$ could in principle explain the excess of noise around 100 Hz, equivalent to a factor of 2.2 higher coating thermal noise (in amplitude) than expected. Note that even including this extra "thermal noise", the expected range should be 81 Mpc. By comparing the accumulated range for the measured curve and this theoretical one, one can deduce that most of the discrepancy (9 Mpc out of 12 Mpc) comes from the "scattering" peaks above 50 Hz (only 59 Mpc are gained above 50 Hz, of the 68 Mpc expected). In other words, even ignoring this "unknown" broadband thermal noise and focusing on fixing the scattering peaks, we should be able to approach 80 Mpc.

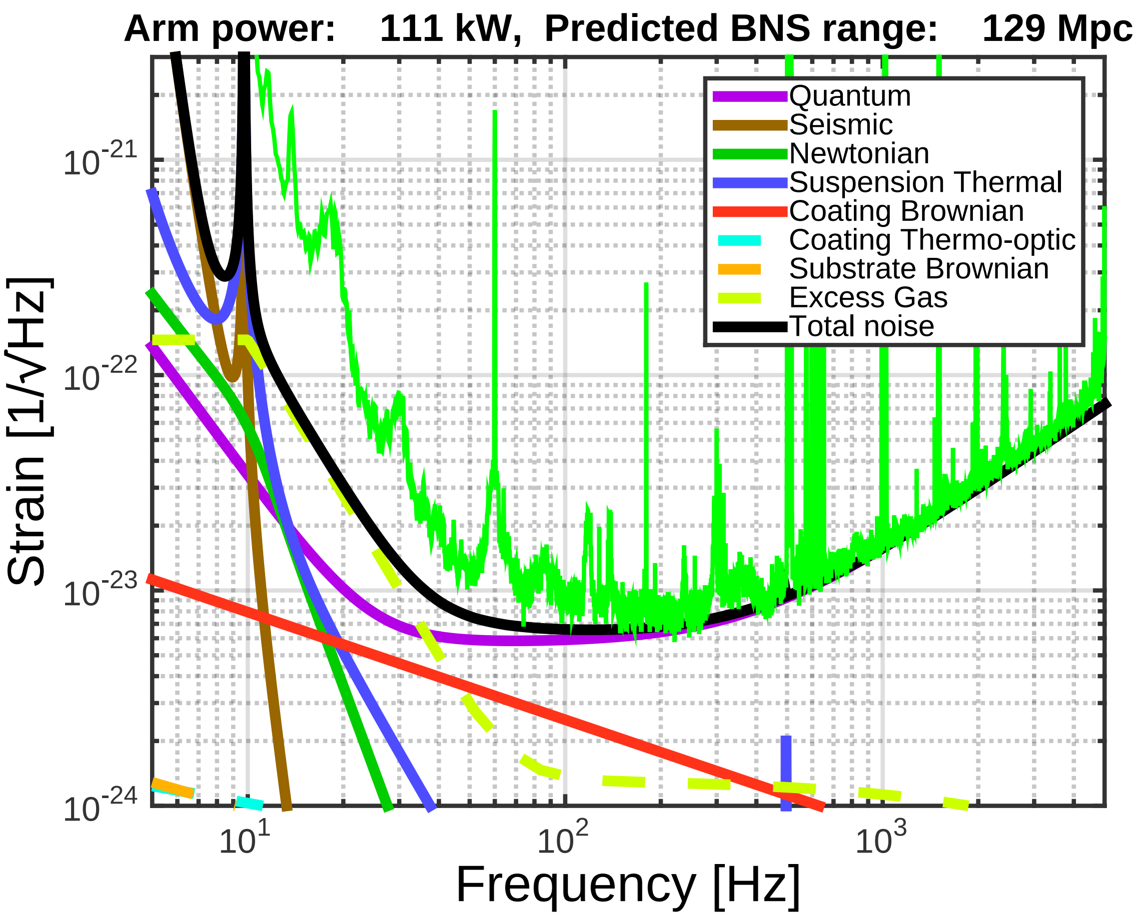

Figure 18: **25W, improved gas thanks to 2 extra pumps.** Prediction based on fundamental noises calculated with GWINC, with the estimated gas noise expected for O1, reduced thanks to the addition of two extra pumps (prediction based on Ryan DeRosa's estimates).

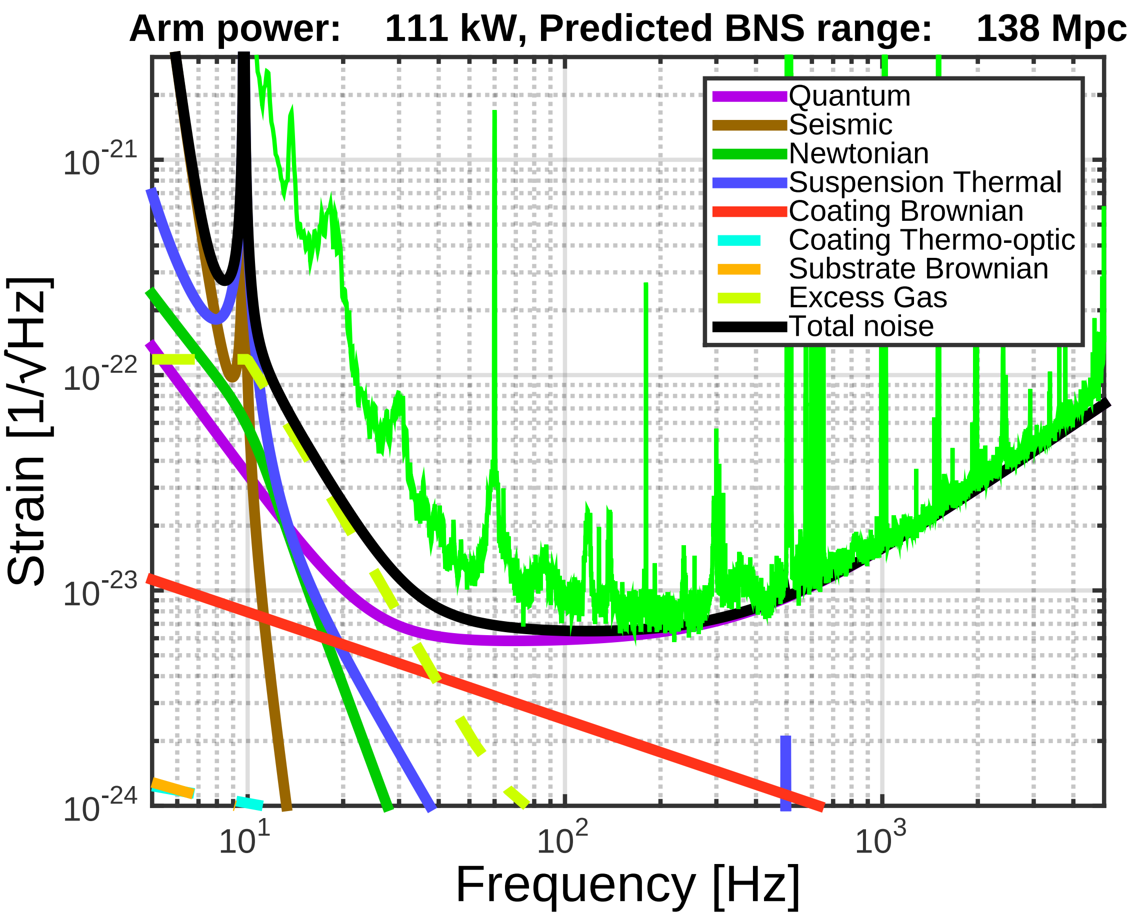

Figure 19: **25W, all new pumps**. Prediction based on fundamental noises calculated with GWINC, with gas noise reduced by the presence of all new pumps (prediction by Ryan DeRosa), corresponding to a theoretical 138 Mpc. By replacing the OMC diodes on top of that, the range would further increase to 143 Mpc.

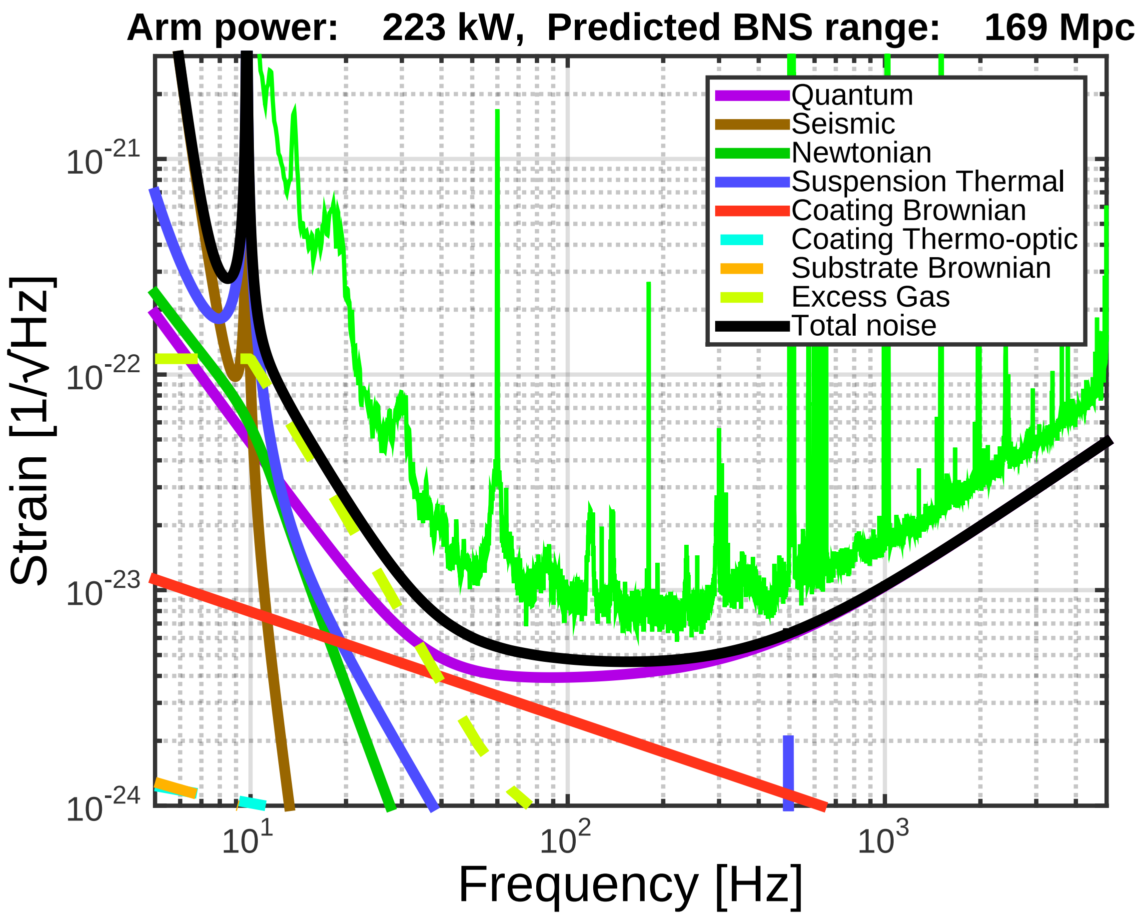

Figure 20: **50W, low gas with all new pumps, better diodes**. Prediction based on fundamental noises calculated with GWINC, assuming that the power is increased by a factor of 2 (from 25W to 50W input delivered by the PSL, corresponding to an intra-cavity increase from 100kW to 200kW) and the quantum efficiency of the photo-detectors is improved by 10% (readout loss reduced from 25% to 15%).

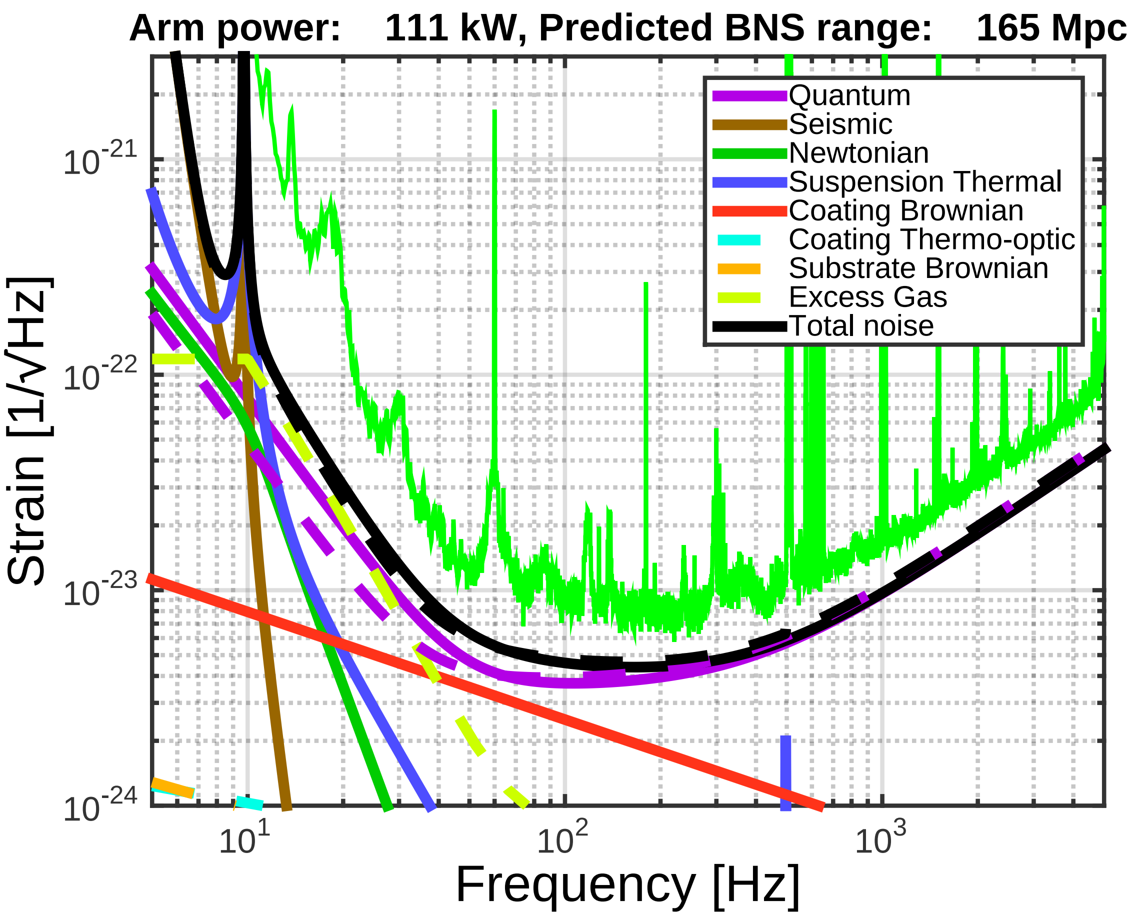

Figure 21: **25W + 8dB injected squeezing, low gas with all new pumps, better diodes.** Prediction based on fundamental noises calculated with GWINC, assuming that the power is not increased above current level (25W from the PSL, 100kW intra-cavity power), the quantum efficiency of the photo-detectors is improved by 10% (readout loss reduced from 25% to 15%), and 20% additional injection loss for the squeezed beam are included. **Dotted lines correspond to quantum and total noise for the 50W**, no squeezing case (figure 20). GWINC output: **You are injecting 8 dB of frequency independent squeezing** Laser Power: 21.25 Watt ifo.Squeezer.InjectionLoss = 0.2; ifo.Optics.PhotoDetectorEfficiency = 1-0.15;

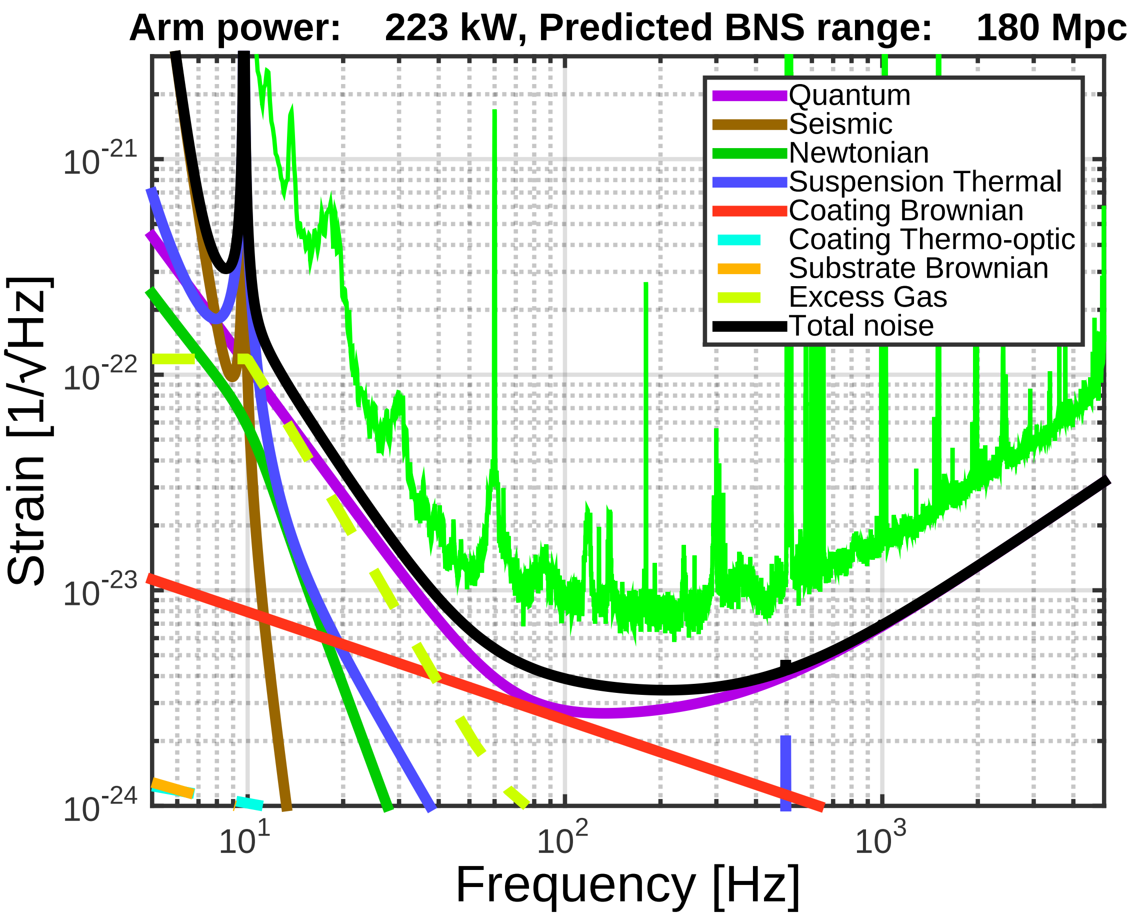

Figure 22: **50W + 8dB injected squeezing, low gas, better diodes.** Prediction based on fundamental noises calculated with GWINC, assuming that the power is not increased above current level (25W from the PSL, 100kW intra-cavity power), the quantum efficiency of the photo-detectors is improved by 10% (readout loss reduced from 25% to 15%), and 20% additional injection loss for the squeezed beam are included. **Dotted lines correspond to quantum and total noise for the 50W**, no squeezing case (figure 20).GWINC output: **You are injecting 8 dB of frequency independent squeezing** Laser Power: 42.50 Watt ifo.Squeezer.InjectionLoss = 0.2; ifo.Optics.PhotoDetectorEfficiency = 1-0.15;

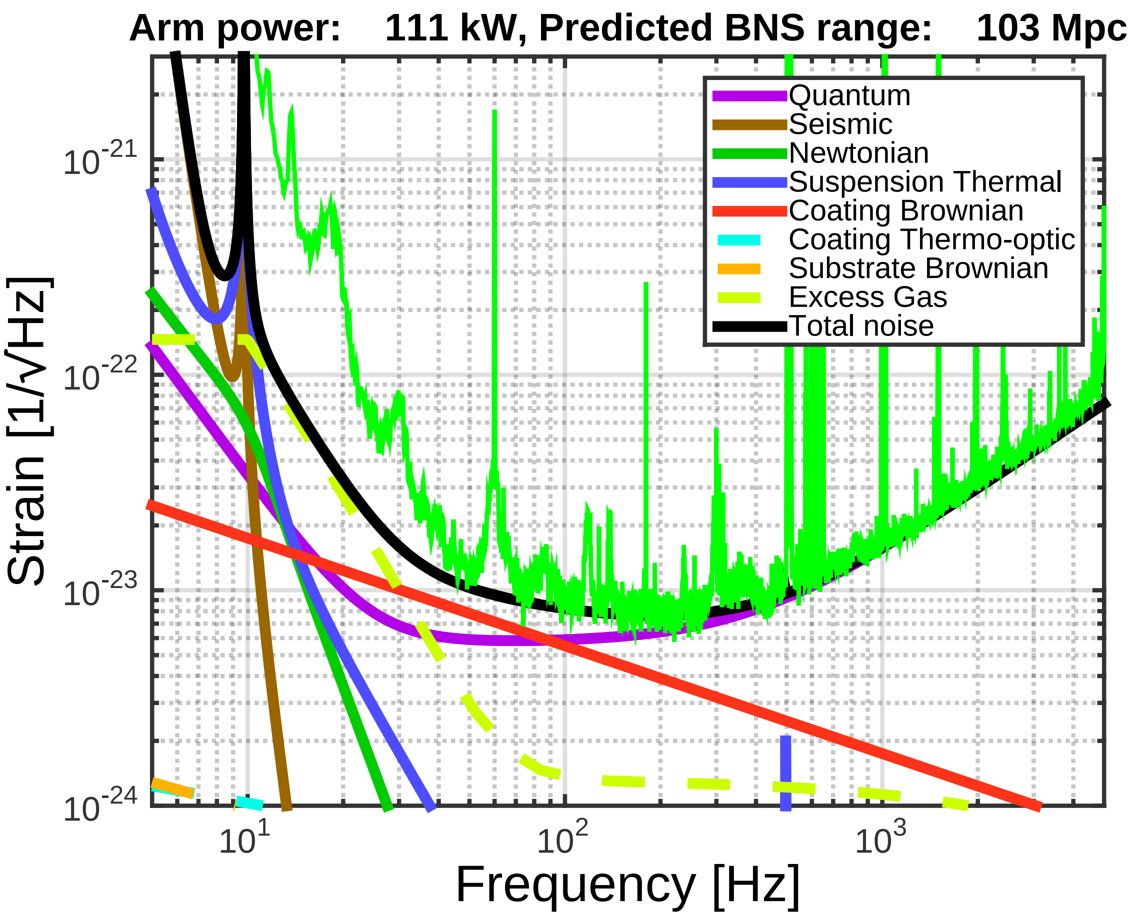

Figure 23: **25W, current gas 2 extra pumps, current excess of "thermal" noise.** Prediction based on fundamental noises calculated with GWINC, assuming the current O1 scenario with gas noise improved by two additional pumps. Note that even with the present unknown broadband extra noise, the predicted range should be around 100 Mpc (compared to 130 Mpc with aLIGO baseline thermal noise, figure 25).

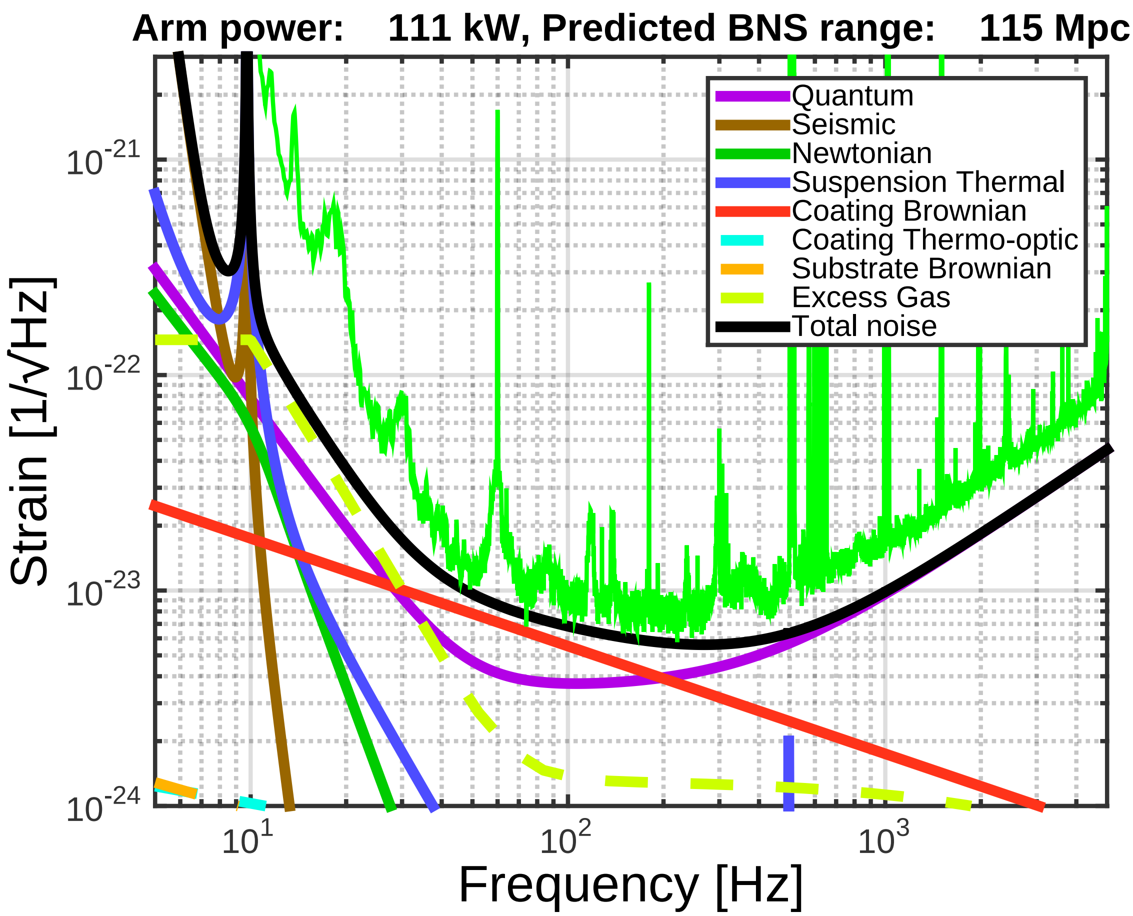

Figure 24: **25W, current gas 2 extra pumps, current excess of "thermal" noise, better diodes, SQZ**. Prediction based on fundamental noises calculated with GWINC, assuming the current O1 scenario with gas noise improved by two additional pumps, the current excess of "thermal" noise, improved diodes and SQZ injection. The predicted sensitivity is 115 Mpc.

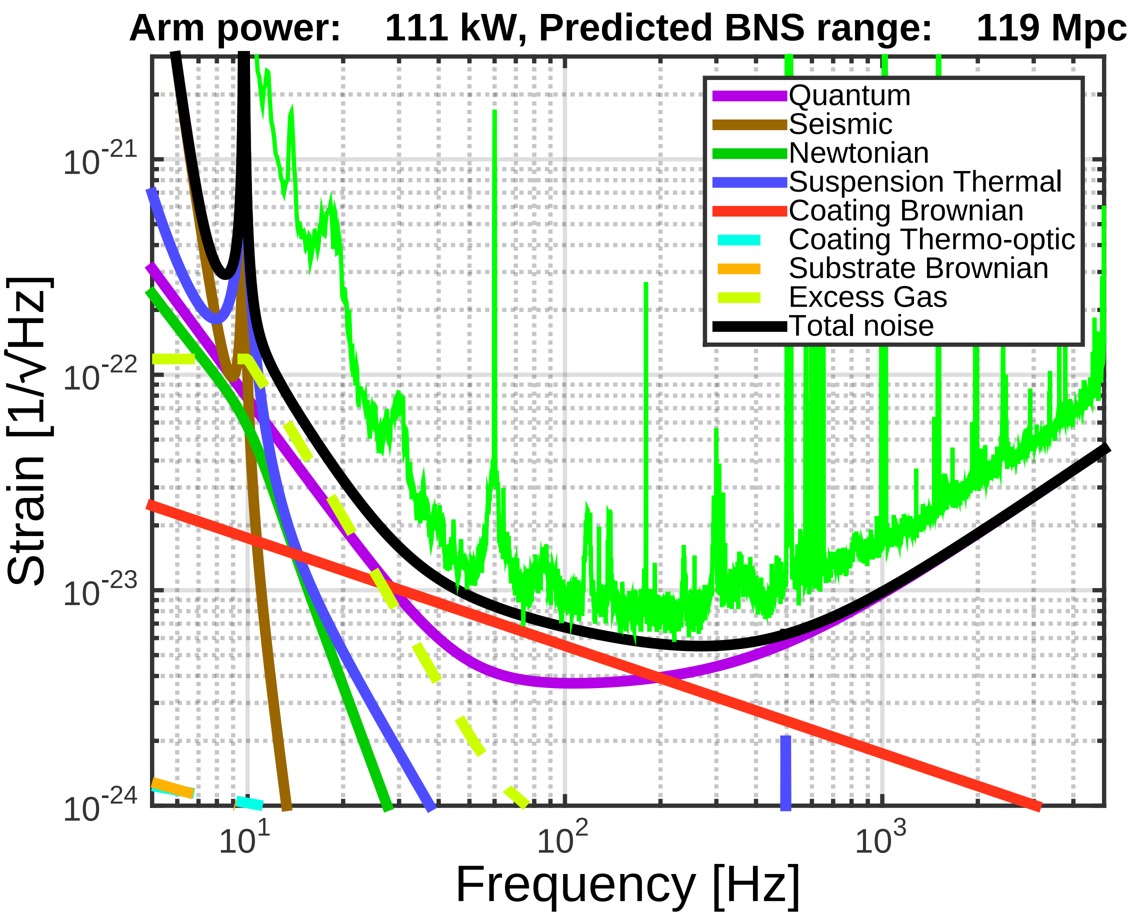

Figure 25: **25W, low gas with all new pumps, current excess of "thermal" noise, better diodes, SQZ.** Prediction based on fundamental noises calculated with GWINC, assuming low gas noise improved by all new pumps, the current excess of "thermal" noise, improved diodes and SQZ injection. The predicted sensitivity is 119 Mpc; so the further improvement of gas noise has little effect in this scenario, as quantum noise limits the sensitivity at low frequency. Coupling low gas noise with higher power, instead of squeezing, will have slightly better impact (122 Mpc, instead of 119 Mpc).

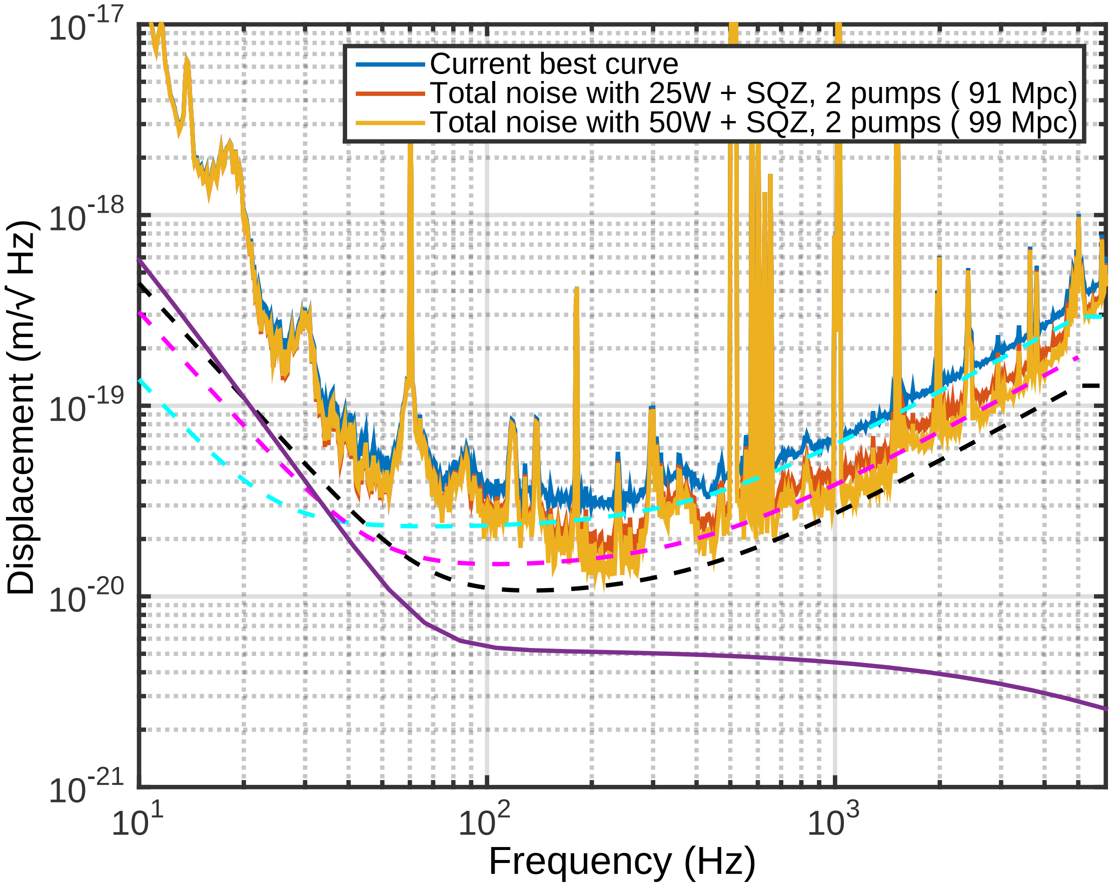

Figure 26: Curves made by starting with the L1 measured curve, subtracting estimate of quantum noise and high gas noise, and replacing them with quantum noise improved by SQZ, and reduced gas noise with 2 pumps.

References

[1] J. Abadie et al., A gravitational wave observatory operating beyond the quantum shot-noise limit. *Nature Physics* **7**, 962 (2011).

[2] J Aasi et al., "Enhanced sensitivity of the LIGO gravitational wave detector by using squeezed states of light", Nature Photon. **7**, 613-619 (2013).

[3] S. Chua, M. Stefszky, C. Mow-Lowry, B. Buchler, S. Dwyer, D. Shaddock, P. Lam, and D. McClelland, Opt. Lett. 36, 4680 (2011).

[4] 99% escape efficiency has been measured in the MIT glass unity, see MIT logbook entry for more details.